FUTURE CIRCULAR COLLIDER STUDY / TECHNIAL PhD REPORT

Description of laboratory analyses performed at the Swiss Federal Institute of Technology (ETH) in Zurich, Switzerland

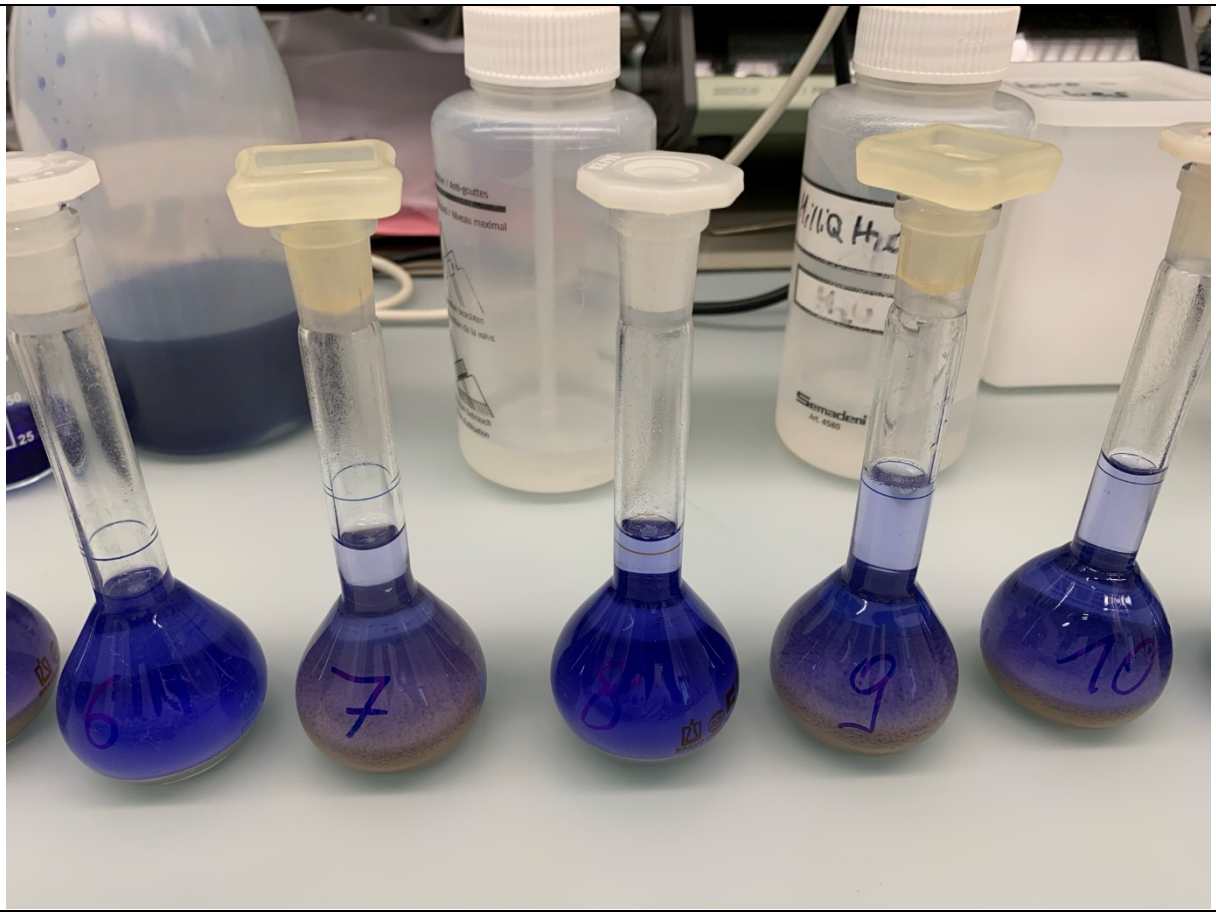

Revision no.	Date	Description	Written by	Edited by	Verified by
0	05/03/2021	Creation of document	Dipl.-Ing. Maximilian Haas		
1	28/03/2021	Revision of document		Dipl.-Ing. Maximilian Haas	
2 (final)	15/04/2021	Review & approval of document			Dr. Michael Plötze

Content

DISCLAIMER

1. Introduction

An essential part of the construction and molasse re-use as part of CERN's Future Circular Collider (FCC) subsurface infrastructure is a thorough understanding of its underlying geology. Hence, rock material has been tested at three distinct laboratories, respectively ETH Zurich, University of Geneva and Montanuniversität Leoben. Based on geomechanical, petrophysical, mineralogical and geochemical laboratory analyses, further implications are derived.
This document describes the laboratory measurements performed at the Eidgenössische Technische Hochschule (ETH) in Zurich, Switzerland from 18 January to 26 February 2021, within the scope of FCC's PhD study on "Geomechanical, petrophysical and sediment-petrographical classification of molasse rock in the Geneva Basin".

The laboratory measurements at the IGT ClayLab, ETH Zurich included:

1. Sample preparation,
2. Water content determination for <63 µm and <400 µm fractions,
3. Leaching characteristics (eluate),
4. Anion analyses,
5. Effective cation exchange capacity (CEC),
6. Exchangeable cations,
7. Fourier Transform Infrared (FTIR) spectroscopy,
8. X-Ray diffraction measurements as powder (XRD-P) and textured (XRD-S) samples,
9. N_2-adsorption for BET surface,
10. Enslin-Neff free water uptake capacity (water absorption),
11. Specific (inner crystalline) surface (water vapour adsorption),
12. Mercury intrusion porosimetry (MIP) and
13. Carbon content determination.

For a detailed scientific description, the reader is referred to literature and technical data sheets cited at the end of each sub-chapter.

This laboratory report is dedicated to methodological descriptions only. Scientific interpretations and further conclusions are stated in the PhD thesis by Maximilian Haas.
For a general overview and further reading about clay analyses and clay minerals, the reader is referred to:

- Bergaya, F. et al. (Eds) (2013): Developments in Clay Science, v5, Handbook of Clay Science. Elsevier
- Jasmund & Lagaly (1993): Tonminerale und Tone: Struktur, Eigenschaften, Anwendungen und Einsatz in Industrie und Umwelt, Steinkopff Verlag Darmstadt (in German).
- Ulery, A.L. & Drees, L.R. (Eds.) 2008: Methods of Soil Analysis. Part 5 – Mineralogical Methods. SSSA Book Series.

2. Sample origin & sample number

Original samples were collected at Swiss (Lucerne) and French (Boussens) core facilities as well as from outcrops along the current FCC subsurface tunnel alignment according to CERN's CDR report (December 2018) featuring samples from Quaternary and Molasse (OSM) formations. Plugs with dimensions of 2-2.5 cm in diameter and 2-8 cm in length were drilled from half cores and outcrop blocks and split in <400 µm, <63 µm and <20 µm fractions for subsequent laboratory analyses. Table 1 gives an overview of the number of samples per analysis.

Table 1: Overview of analyses at the IGT ClayLab, ETH Zurich.

type of analysis	sample amount	sample location (wells & outcrops)
ICP-OES	74	Point 1, Geo-02, Peissy-I, Sarzin, Mornex, GEX-CD-4, GEX-CD-5, GEX-CD-7
CEC	76	
ICP-CEC	76	
Cuvette tests	42	
FTIR	31	
XRD	79	
BET surface	30	
Water vapour adsorption	59	
MIP	30	
Enslin-Neff	70	
Carbon content	70	

3. Sample preparation

Sample preparation was performed on drilled plugs starting with different milling devices to gain respective grain size fractions. After completion of milling, each sample has been dried to determine water content required as input for further calculations.

3.1. Milling of samples

As a first step, a jaw crusher was used to receive a fraction <400 µm for each sample. Second, an agate mill crushed the sample down to a fraction of <63 µm. For the FTIR and XRD measurements, a very fine-grained material (<20 µm) was necessary leading to a third milling step of milling the <400 µm fraction in a vibrating McCrone mill, flushing them with ethanol and drying the sample-ethanol solution in a 65 °C oven between 2 to 5 hours depending on solution volume to receive a <20 µm fraction. For the <400 µm and <63 µm fractions, respective sieves are used to check the grain sizes after each milling step.

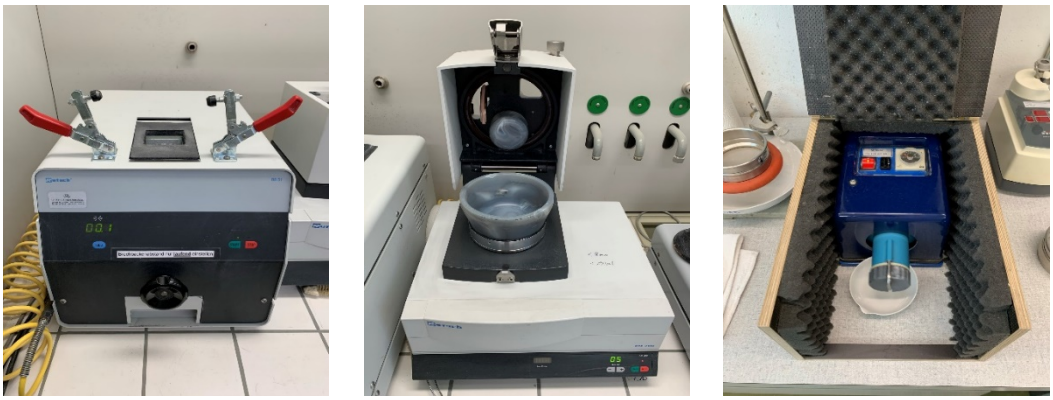

Figure 1: Overview of mills used for sample preparation. Left: jaw crusher for fraction <400 µm, middle: agate mill for fraction <63 µm, right: vibrating McCrone mill for fraction <20 µm.

3.2. H_2O content via 105 °C drying

For fractions <400 µm and <63 µm the water content was determined after DIN EN 12880, DIN EN ISO 17892-1 and DIN 18121-1 to calculate the dry mass. This excludes measurements for XRD and FT-IR using the <20 µm fraction as these analyses do not require dry mass input. The water content using humid and dry masses is calculated according to:

$$w(\%) = \frac{m_{humid} - m_{dry}}{m_{humid}} \cdot 100$$

Each sample was dried for 48h in a 105 °C oven until mass equilibrium. The present molasse samples showed rather low water contents ranging from 0.4 to 5.15 %.

4. Leaching characteristics (eluate) via ICP-OES

Inductively Coupled Plasma Optical Emission Spectrometry (ICP-OES) is a simple and high-precision state-of-the-art device for leaching (eluate) analyses, and successively supersedes the atomic absorption spectroscopy (AAS) analysis.
The measurements were performed using an Agilent 5110 ICP-OES device and followed DIN EN 12457-2 (leachate characterization waste), with minor changes made with respect to water content corrections and initial dry masses for the eluate solution/dry mass ratio. Each sample was measured for 20 s after 5 s stabilization time using a RF power of 1.2 KW in axial

viewing mode with 8 mm viewing height and a plasma flow of 12 L/min. For each sample run, a blank sample and 4 standards have been used for calibration, followed by a quality control spike blank sample. The optimal ratio of eluate-dry mass according to the DIN standard should not exceed 10, which resulted in initial weights of 5 g of a <400 µm sample.

Results are given in mg/L and calculated according to DIN EN 12457-2:

$$A = C \cdot \left(\frac{L}{M_T} + \frac{FG}{100}\right)$$

With:
A = leaching substance at L/S ratio = 10, in mg/kg dry mass,
C = concentration of certain part in eluate solution, in mg/L,
L = volume leaching conditioning substance, in L,
FG = humid mass, in percentage related to dry mass.
M_T = dry mass of sample, in kg.

References & further reading:

- Leachate characterization waste, DIN EN 12457-2, https://www.beuth.de/de/norm/din-en-12457-2/52065709.

5. Anion analyses via cuvette tests

According to Swiss and French disposal classes (e.g. Ordinance on the Avoidance and the Disposal of Waste, version 01.01.2021) specific anions must not exceed legal thresholds as indicated in respective documents. While the ICP-OES method (see section 7) allowed the quantification of most cations, complementary anion analyses were performed as indicated in Table 2. For each anion, the company Hach Lange provides standardised cuvette tests in combination with its Spectral-Photometer DR 6000 (see section 5) analysed photometrically.

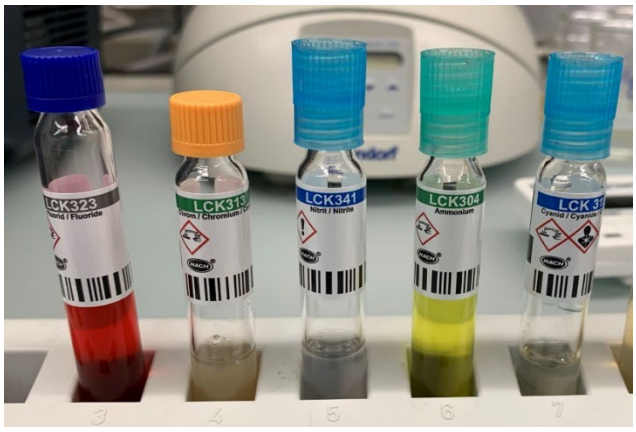

Figure 2: Overview of performed cuvette tests.

Table 2: Overview of measured anions complemented by ICP-OES analysis.

test-ID	parameter	measuring range	method	standard
LCK323	Fluoride, F^-	0.1 - 2.5 mg/L	SPADNS	-
LCK315	Cyanide free, CN^-	0.01 - 0.6 mg/L	Babituric Acid-Pyridine	-

LCK341	Nitrite, NO^{2-}-N	0.015 - 0.6 mg/L	Diazotisation	EN ISO 26777, DIN 38405 D10
LCK304	Ammonium, NH_4-N	0.015 - 2.0 mg/L	Indophenol Blue	ISO 7150-1, DIN 38406 E5-1, UNI 11669:2017
LCK313	Chromium-VI	0.03 - 1.0 mg/L	Diphenylcarbazide	EN ISO 11083, DIN 38405-D24

References & further reading:

- Hach LCK Cuvette Test System, Technical Data Sheet.
- Ordinance on the Avoidance and the Disposal of Waste, version 01.01.2021, https://www.fedlex.admin.ch/eli/cc/2015/891/en

6. Effective CEC via $[Cu(trien)_3]^{2+}$ complex

The cation exchange capacity (CEC) via $[Cu(trien)_3]^{2+}$ complex analyses effective cation exchange capacity of clay minerals at pH of 7-8 based on the method proposed by Meier & Kahr (1999). The sample solution was mixed with a $[Cu(trien)_3]^{2+}$ complex and analysed via photometry to conclude on effective exchangeable cations in meq/100g.
800 mg of a <63 µm milled sample were treated in the ultrasound UP 200H device for 3 minutes to separate the clay minerals and destroy clay aggregates. The remaining volume was filled up with millipore-H_2O. Each sample was shaken overhead 30 times and left for sedimentation and exchange for about 1-2 hours. After sedimentation, solution was filled into a centrifuge cup, which rotated at 13,000 RPM for 20 minutes in the Eppendorf Minispin centrifuge. Finally, the centrifuged solution was pipetted into the sample holder cuvette and analysed in the Spectral-Photometer DR 6000 by Hach Lange.
Calibration, i.e. determination of analysing wavelength was performed using a blind sample (millipore-H_2O).

Figure 4: Required measurement devices for CEC determination. Left: Spectral-Photometer DR 6000 by Hach Lange, middle: Eppendorf MiniSpin centrifuge, right: ultrasonic UP 200H.

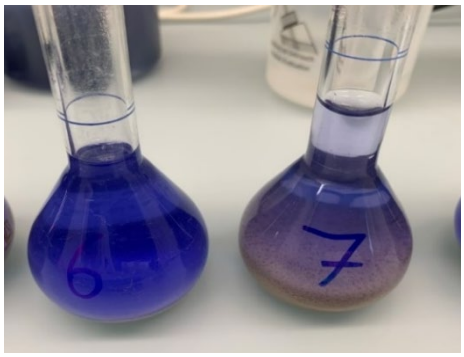

Figure 3: Left sample depicting a low CEC compared to high CEC on right sample.

Wavelength at maximum extinction was given at 278.00 nm for the present samples, and the zero-baseline was set before running actual sample measurements. Effective CEC was then calculated according to:

$$\mathrm{CEC}(mmol/100gclay) = \frac{\left(Ext._{blind} - Ext._{sample}\right) \cdot 200 \cdot 100}{m_{sample}}$$

With:

- $Ext._{blind}$ & $Ext._{sample}$ = respective extinction values in nm of the blind and real sample,
- m_{sample} = sample mass in gram.

The calculation was corrected by the <63 µm fraction H_2O content for dry mass.

References & further reading:

- Meier, L.P., Kahr, G., 1999. Determination of the Cation Exchange Capacity (CEC) of Clay Minerals Using the Complexes of Copper(II) Ion with Triethylenetetramine and Tetraethylenepentamine. Clays Clay Miner. 47, 386–388.

7. Exchangeable cation analyses via ICP-OES

By measuring the copper-II-complex solution after cation exchange (see section 6), exchangeable cations are quantified via Inductively Coupled Plasma Optical Emission Spectrometry (ICP-OES). The same Agilent 5110 ICP-OES device was used as for the leaching analyses. Condition settings were adapted accordingly to 10 s of reading time and 15 s stabilization time. Viewing mode was changed to radial with a viewing height of 15 mm. Same settings for RF power were applied as for the leaching analyses. For each sample run, a blank sample and 3 standards have been used for calibration, followed by a quality control spike blank sample and a copper blank sample. Apart from a different centrifuge speed of 4,500 RPM in the Heraeus centrifuge, the same sample preparation procedure as for the ICP-eluate analysis (see section 4) was applied. Hence, sample preparation started with the CEC copper-II-complex solution being filtered with <0.45 µm PES vaccine filters and acidized with 2 % HNO_3.

References & further reading:

- Gaines, G.L., Thomas, H.C., 1953. Adsorption Studies on Clay Minerals. II. A Formulation of the Thermodynamics of Exchange Adsorption. J. Chem. Phys. 21.
- Harland, C.E., 1994. Ion Exchange, RSC Paperbacks. The Royal Society of Chemistry.
- Meier, L.P., Kahr, G., 1999. Determination of the Cation Exchange Capacity (CEC) of Clay Minerals Using the Complexes of Copper(II) Ion with Triethylenetetramine and Tetraethylenepentamine. Clays Clay Miner. 47, 386–388.
- Bergaya F, Lagaly, G., Vayer M.: Cation and Anion Exchange. In: Handbook of Clay Science (Eds. Bergaya, Theng, Lagaly) Developments in Clay Science Vol. 1, pp. 979-1001 and references therein.

8. Mineralogical analyses via FTIR and XRD

8.1. *Fourier Transform Infrared spectroscopy (FTIR)*

The FTIR spectroscopy derives mid-infrared spectra based on measured interferograms following Lambert-Beer's law. These interferograms are Fourier-transformed from time into frequency domain and allow conclusions about organic material as well as amorphous and crystallized mineral phases. The resulting spectra are displayed along 450 to 4000 cm^{-1} (wavenumber, x-axis) versus percentage of transmission (%T, y-axis).

Figure 5: Tools required for FTIR sample preparation. Left: agate mortar, funnel and desiccator (for sample conservation), middle: 1 mg of sample mixed with 199 mg KBr, right: pressing apparatus applying 10 tons onto the sample resulting in the pressed KBr pill.

A KBr (potassium-bromide) disc was prepared with 1 mg sample material <20 µm dried at 105 °C dispersed in 199 mg KBr. The spectra were measured with a Perkin Elmer Spectrum One device using the program Spectrum V5.3.1. Each analysis measured 20 runs and was summed up to a transmission spectrum.

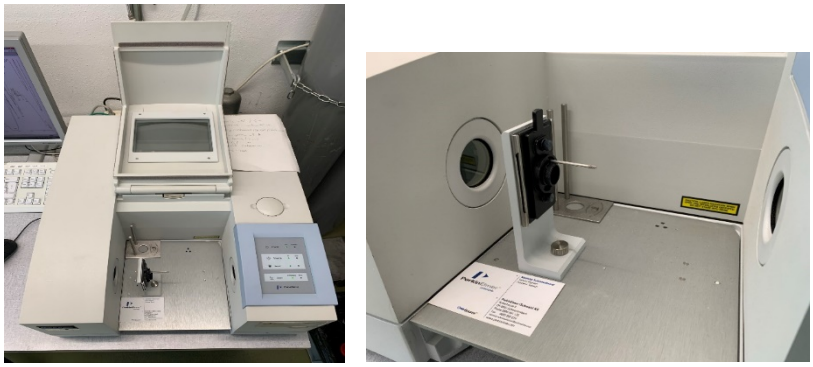

Figure 6: Left: Perkin Elmer Spectrum One FTIR device used for analysis, right: close-up of sample holder inside the measuring device when turned

References & further reading:

- Farmer, V.C., 1974. The Infrared Spectra of Minerals. MinSoc Monograph 4.
- Van der Marel H.W., Beutelspacher H. 1976. Atlas of Infrared Spectroscopy of Clay Minerals and their Admixtures. Elsevier, Amsterdam.
- Smykatz-Kloss, W., Warne, S.S.J. (Eds.) 1991. Thermal Analysis in the Geosciences. Springer.
- Christidis, G.E. (Ed.) Advances in the Characterization of Industrial Minerals. EMU Notes in Mineralogy v9. Chapter 6: Madejova, J. et al. Application of vibrational spectroscopy to the characterization of phyllosilicates and other industrial minerals.

8.2. X-Ray diffraction (XRD)

X-Ray diffraction (XRD) is the most common method to determine crystalline mineral phases qualitatively and quantitatively. The method was applied according to standard DIN EN 13925-1/-2. Two different types of samples were prepared and measured with a D8 Advance Bruker AXS/D XRD device. For quantitative XRD analyses, randomly oriented (Zhang et al., 2003) Ca-exchanged samples were scanned from 4 to 80° 2θ with steps of 0.02° 2θ at 2 s intervals using a Bragg-Brentano X-ray diffractometer (Bruker AXS D8 Advance, Germany). Oriented specimens were used for enhancement of the basal reflexes of layer silicates thereby facilitating their identification. The changes in the reflex positions in the XRD pattern by intercalation of different organic compounds (e.g. ethylene glycol) and after heating were used for identification in part of smectite. The XRD instrument worked with CoKα-radiation generated at 35 kV and 40 mA, and with dynamic beam optimisation using an automatic theta compensating divergence slit and a motorised anti-scatter screen. The diffractometer was equipped with primary and secondary soller slits, and an energy dispersive LynxEye XE-T line detector. Qualitative phase analysis was analysed with the software DIFFRAC.EVA v4.3 (Bruker AXS). The minerals were identified by peak positions and relative intensities in the X-ray diffraction pattern compared with the PDF2 database (ICDD 1998). Quantitative mineral analyses were performed with Rietveld analysis of the XRD patterns using the program Profex/BGMN V4.2.4 (Döbelin and Kleeberg, 2015). This full pattern-fitting method calculates X-ray diffraction pattern based on crystallographic data of each mineral phase and its iterative adjustment (least-square fit) to the measured diffractogram. In the refinement, phase specific parameters and the phase content were adapted to minimize the difference between the calculated and the measured X-ray diffractogram.

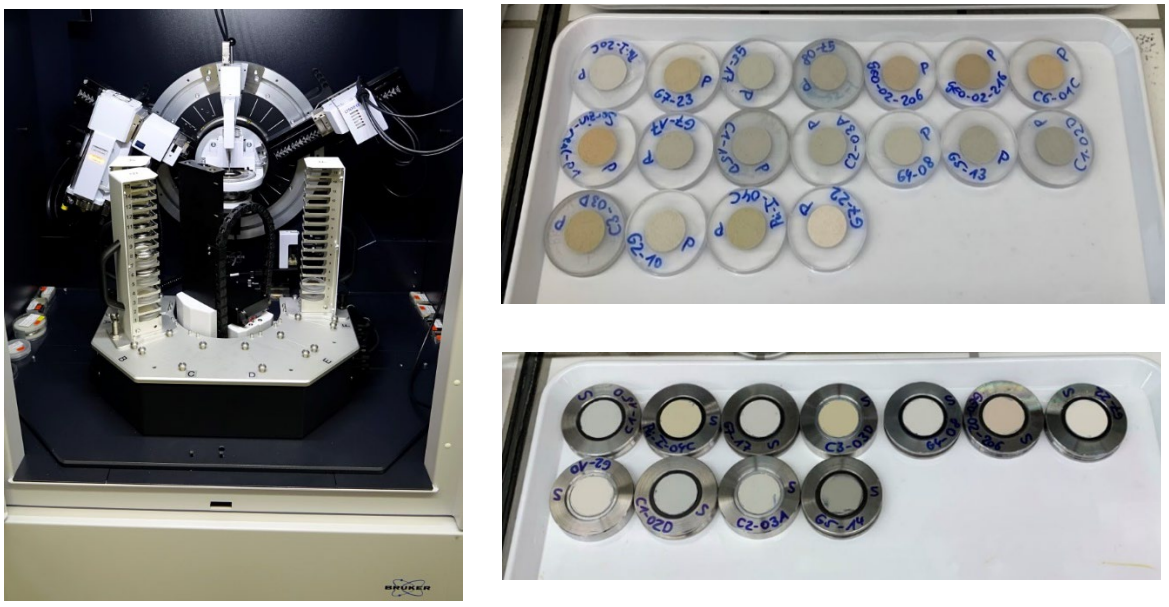

Figure 7: Left: XRD-device, right top: Powder (XRD-P) samples used for bulk analysis (Rietveld), right bottom: textured (XRD-S) samples used for clay mineral identification.

References & further reading:

- Moore, D.M., Reynolds, R.C., 1989. X-ray Diffraction and the Identification and Analysis of Clay Minerals, Clays and Clay Minerals. Oxford University Press.
- Döbelin, N., Kleeberg, R., „Profex: a graphical user interface for the Rietveld refinement program BGMN„, Journal of Applied Crystallography 48 (2015), 1573-1580.
- Christidis, G.E. (Ed.) Advances in the Characterization of Industrial Minerals. EMU Notes in Mineralogy v9. Chapter 3: Bish D., Plötze, M. X-ray powder diffraction with emphasis on qualitative and quantitative analysis in industrial mineralogy.

9. Surface analyses via gas adsorption

9.1. N_2-BET surface adsorption

The method after DIN ISO 9277 measures specific surfaces via N_2 gas adsorption. Analysis preparation took about 1 day, while the second day was dedicated to actual sample measurement. On day one, the 150 °C dried sample was weighed in a sample tube, whose end was attached to a VacPrep 061 vacuum pump. Heating elements increased temperature gradually starting at 25 °C up to 150 °C and the sample was subjected to 150 °C for 15 h. Then, the sample tube was flushed with nitrogen gas for about 30 seconds at 0.5 bar. Afterwards, the sample was weighed on a medium-precision scale with 4 digits, and placed in the Quantachrome Autosorb-1^{MP} N_2-adsorption measurement device for sample analysis.

Figure 8: Left: VacPrep 061 vacuum pump used for sample degassing, middle: Quantachrome Autosorb-1 device for measuring specific (outer) surface, right: close-up of liquid nitrogen tank, in which sample is immersed.

Data processing and analysis was performed using the ASiQwin Version 3.01 software applying the multipoint BET method (nitrogen on silicates as adsorbate), which included 11 points in a relative p/p_0 range of 0.1 to 0.3 to calculate specific surfaces.

References & further reading:

- Brunauer, S., Emmett, P.H., Teller, E., 1938. Adsorption of Gases in Multimolecular Layers. J. Am. Chem. Soc. 60, 309–319.
- Madsen, F.T., Kahr, G., 1992. Wasserdampfadsorption und spezifische Oberfläche von Tonen, in: Graf v. Reichenbach, H. (Hrsg.): Hydratation Und Dehydratation von Tonmineralen - Beiträge Zur Jahrestagung Hannover, DTTG. p. 8.
- Lowell, S., Shields, J.E., Thomas, M.A., Thommes, M. 2004: Characterization of porous solids and powders: surface area, pore size and density. Kluwer Academic, Dordrecht.
- Gregg, S.J., Sing, K.S.W. 1982: Adsorption, Surface Area and Porosity. Academic Press, London.

9.2. Water vapour adsorption

Vapor adsorption after Keeling et al. (1980) provides insights about the specific inner crystalline surface of clay minerals, respectively their water adsorption behaviour adsorbing H_2O molecules between their layers. The combination of Enslin-Neff (see section 10), BET and Keeling analyses provides powerful insights about a rock's water behaviour, respectively swelling potential. The latter further allows reasonable correlations with CEC (see section 6).

Figure 9: 75% RH conditions for 3 continuous weeks.

A <63 µm sample of 4 g was placed in a container with 75% relative humidity (RH) achieved above an oversaturated NaCl solution under atmospheric pressure. The sample's initial weight was compared to its conditioned and fully dried weight. Random samples were checked occasionally within 2-3 days for mass equilibrium after three weeks. Once no further adsorption was encountered, samples were weighted on a high-precision 5-digit scale. Afterwards, the sample was dried for 1 week in a 105 °C oven. The difference of humid, 75% RH adsorbed and dried masses (in mg) yielded the water adsorption according to:

$$w_{adsorption}(\%) = \frac{m_{75\%RH} - m_{dry}}{m_{dry} - m_{glass}} \cdot 100$$

References & further reading:

- Keeling, P.S., Kirby, E.C., Robertson, R.H.S., 1980. Moisture adsorption and specific surface area. J. Brit. Ceram. Soc. 79, 36–40.
- Madsen, F.T., Kahr, G., 1992. Wasserdampfadsorption und spezifische Oberfläche von Tonen, in: Graf v. Reichenbach, H. (Hrsg.): Hydratation Und Dehydratation von Tonmineralen - Beiträge Zur Jahrestagung Hannover, DTTG. p. 8.
- Lowell, S., Shields, J.E., Thomas, M.A., Thommes, M. 2004: Characterization of porous solids and powders: surface area, pore size and density. Kluwer Academic, Dordrecht.

- Gregg, S.J., Sing, K.S.W. 1982: Adsorption, Surface Area and Porosity. Academic Press, London.

10. Water absorption via Enslin-Neff

The Enslin-Neff analysis measures the water uptake capacity under free swelling conditions and its associated time evolution of rock-water interaction according to standard DIN 18132. About 1 g of a <400 µm sample was placed in the Enslin-Neff apparatus and its free water uptake capacity was recorded in a time interval of 0.25, 0.5, 1, 2, 4, 8, 15, 30, 60, 120, 240, 360 and 1440 minutes. Once the material reached its maximum absorption, the analysis was stopped, and water absorption was calculated according to:

$$w_a(\%) = \frac{w_{max}}{m_{dry} \cdot 100wt\%}$$

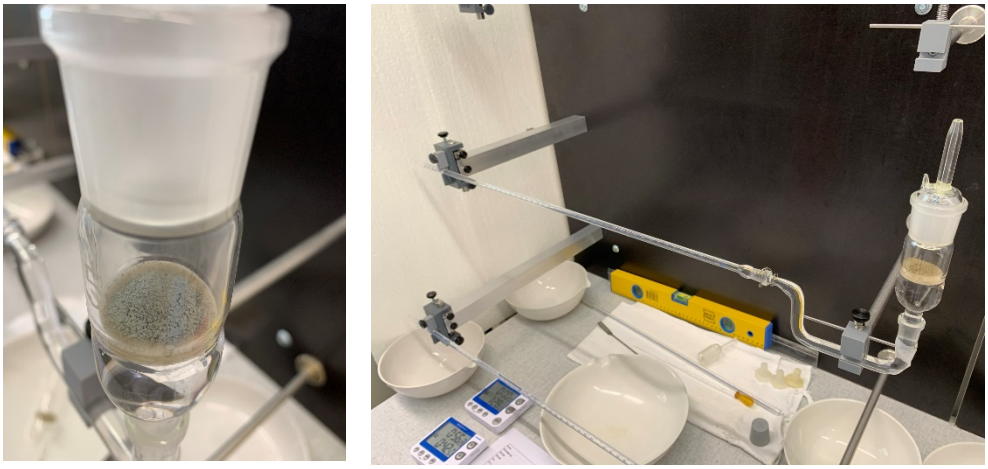

Figure 10: Left: close-up of sample burette with sample powder during water uptake, right: full Enslin-Neff apparatus including scaling burette to read absorbed water in ml.

References & further reading:

Kaufhold, S., Dohrmann, R., 2008. Comparison of the traditional Enslin-Neff method and the modified dieng method for measuring water-uptake capacity. Clays Clay Miner. 56, 686–692.

- Kugler, H., Schwaighofer, B., Gruber, S., 2002. Die Modifizierung des Wasseraufnahmeversuches nach Enslin-Neff, in: Ottner, F., Gier, S. (Hrsg.): Beiträge Zur Jahrestagung Wien, Berichte Der DTTG, Band 9. p. 9.
- Neff. H., 1959. Über die Messung der Wasseraufnahme ungleichförmiger bindiger anorganischer Bodenarten in einer neuen Ausführung des Enslingerätes. Die Bautechnik 11, 10.
- Neff, H.K., 2005. Der Wasseraufnahmeversuch nach ENSLIN-NEFF in der erd- und grundbautechnischen Praxis, in: 5. Österreichische Geotechniktagung. 21.02. & 22.02.2005, Vienna, p. 27.

- Demberg, W. 1991: Über die Ermittlung des Wasseraufnahmevermögens feinkörniger Böden mit dem Gerät nach Enslin/Neff. Geotechnik 14, 125-131.
- Enslin-Neff apparatus after DIN 18132.

11. Pore size distribution & porosity analysis via mercury intrusion

The mercury intrusion porosimetry measures effective, total (i.e. non accessible pores) porosity and pore size distribution according to standard ISO 15901-1. To cover the full range of pore sizes, two POROTEC PASCAL devices with different pressure ranges were used. The low-pressure device used up to 400 kPa to inject mercury into the sample, while the high-pressure device used up to 400 MPa and high-pressure oil to further induce the mercury into the smallest pores down to 2 nm radius.

Figure 11: Low- and high-pressure chambers to analyse porosity and pore size distribution. Right: low-pressure device for mercury intrusion, left: high-pressure device to further induce the mercury into nanometer pores using high-pressure

The samples were weighed into a dilatometer flask and evacuated in the macropore unit of the pressure porosimeter for 10 min. The dilatometer flask was filled with mercury under vacuum up to a certain volume in the measuring capillary. Then, the pressure of the low-pressure device was slowly increased up to 400 kPa. The dilatometer flask was removed from the macropore unit at air-out pressure, weighed and placed in the micropore unit of the pressure porosimeter. The pressure on mercury fluid in the dilatometer was gradually increased to 400 MPa in the second high-pressure device using a special oil in the autoclave of the micropore unit. As the pressure increases, the mercury intruded into smaller pores. The pore volume was derived from the amount of mercury intruded. The pore size distribution was determined according to the equation stated by Washburn (1921):

$$r = \frac{-2\gamma cos(\theta)}{p}$$

With:
γ = mercury surface tension,
p = applied, absolute pressure,
r = pore radius,
θ = wetting angle.

Figure 12: Transfer of mercury injected sample from low-pressure to high-pressure device.

Assuming a mercury surface tension of 4800 N/m, a wetting angle for mercury of 141.3° and cylindrical pore shape, this results in the following equation:

$$r = \frac{7500}{p}$$

With:
r = pore radius in nm,
p = applied absolute pressure in kg/cm^2.

References & further reading:

- Washburn EW (1921) Note on a method of determining the distribution of pore sizes in a porous material. Proc Natl Acad Sci 7:115–116
- Giesche, H. 2006. Mercury Porosimetry: a General (Practical) Overview. Part. Part.Syst. Charact. 23, 1-11.
- Scrimgeour, C., 2008. Soil Sampling and Methods of Analysis (Second Edition), 2008/07/01. ed, Experimental Agriculture. Cambridge University Press.
- Kaufhold et al. 2016. Comparison of methods for the determination of the pore system of a potential German gas shale. CMS workshop lecture series vol21, ch13, 163-190. .

12. Carbon content determination via acid and thermal treatment

The total carbon (TC) and total inorganic carbon (TIC) methods were performed according to DIN EN 15936 in a multi-EA 4000 device and allowed conclusions about carbon content. For TC and TIC analyses, a 105 °C dried <400 µm sample was split into two sub-samples of different initial weight, respectively 50 mg for TIC and 300 mg for TC analysis. A $CaCO_3$ reference sample was used as a standard for all analyses. For the TIC analysis, the sub-sample was subjected to 35 % H_3PO_4 acid and released CO_2 gas was detected via non-dispersive infrared (NDIR), which was used to calculate TIC content. For the TC content, the sub-sample was burned in a 1300 °C oven and release of CO_2 was detected by NDIR. The total organic carbon (TOC) content was then derived indirectly via the difference method subtracting TIC from TC content in the multi-EA Analytik Jena software.

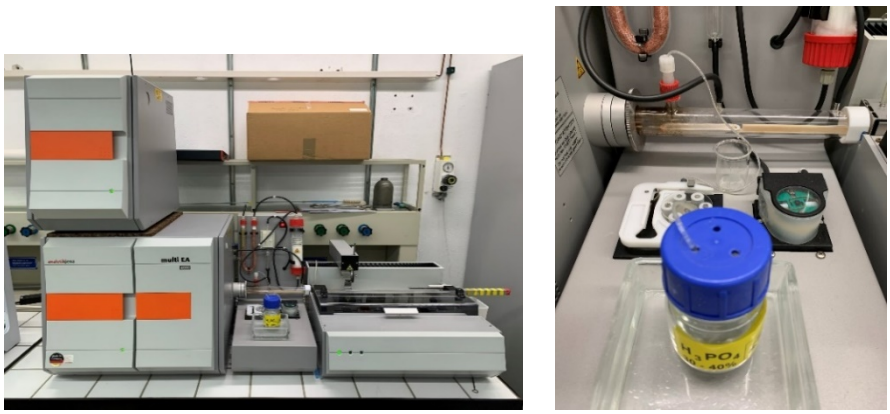

Figure 13: Left: Determination of carbon content with multi EA 4000 device, right: close-up of TIC determination with H_3PO_4.

References & further reading:

- DIN-EN-15936 for carbon determination, https://www.beuth.de/en/standard/din-en-15936/149052152